A real-time approach to robust identification of tire-road friction characteristics on mixed-μ roads

Mojtaba Sharifzadeh[a], Adolfo Senatore[a], Arash Farnam[c], Ahmad Akbari[b], and Francesco Timpone[d*]

[a]*Department of Industrial Engineering, University of Salerno, Italy.* {*a.senatore, msharifzadeh*}*@unisa.it ;* [b]*Institute of Automatic Control, Sahand University of Technology, Tabriz, Iran. a.akbari@sut.ac.ir;* [c]*Data Science Lab, Faculty of Engineering and Architecture, Ghent University, Ghent, Belgium. arash.farnam@ugent.be;* [d]*Department of Industrial Engineering, University of Naples Federico II, Naples, Italy. francesco.timpone@unina.it*

The interaction between the tire and the road is crucial for understanding the dynamic behavior of a vehicle. The road-tire friction characteristics play a key role in the design of braking, traction, and stability control systems. Thus, in order to have a good performance of vehicle dynamic stability control, real-time estimation of the tire-road friction coefficient is required. This paper presents a new development of an on-line tire-road friction parameters estimation methodology and its implementation using both LuGre and Burckhardt tire-road friction models. The proposed method provides the capability to observe the tire-road friction coefficient directly using measurable signals in real-time. In the first step of our approach, the recursive least squares is employed to identify the linear parameterisation (LP) form of Burckhardt model. The identified parameters provide through a T-S fuzzy system the initial values for the LuGre model. Then a new LuGre model-based nonlinear least squares (NLLS) parameter estimation algorithm using the proposed static form of the LuGre to obtain the parameters of LuGre model based on recursive nonlinear optimization of the curve fitting errors, is presented. The effectiveness and performance of the algorithm are demonstrated through the real time model simulations with different longitudinal speeds and different kinds of tire on various road surface conditions in both Matlab/Carsim environments as well as collected data from real experiments on a commercial trailer.

Keywords: Nonlinear least squares (NLLS) identification; recursive estimation; Burckhradt & LuGre friction models; longitudinal vehicle dynamics

1. Introduction

Since the motion of a ground vehicle is primarily determined by the friction forces transferred from roads via tires, information about the tire/road friction is critical for many active vehicle safety control systems, including longitudinal control, yaw stability control and rollover prevention control systems. In particular friction formation, is a crucial tool for Brake Assist Systems (BAS), Electronic Stability Control (ESC-ESP) and Adaptive Cruise Control (ACC) systems that have recently become essential for active safety systems [1, 2]. For instance, in the case of adaptive cruise control, estimation of friction coefficient (μ) enables the braking distances to be adjusted in real time (see e.g. [3]).

---
*Francesco Timpone. Email: francesco.timpone@unina.it

Many research papers dealing with stability monitoring and control have also proposed the explicit use of friction coefficient information in their various calculations [4]. It has also been demonstrated that if this real-time information is automatically identified and vehicle control and intelligent strategies are adjusted according to the identified results, this can mainly enhance the vehicle safety performance undoubtedly.

With this description the real-time estimation of the tire-road friction characteristics on roads with inhomogeneous friction properties (mixed-μ roads) is of fundamental importance in each active safety system and thus this issue has been even more important in recent years. Unlike other easily measurable parameters, such as the wheel angular speeds, vehicle acceleration and wheel load, there is currently no economically feasible sensor that can be installed in the vehicle to measure the friction parameters. Because many factors affect road friction coefficient, such as road surface conditions, tire types, vehicle and wheel velocity [5], the adaptive identification of maximum friction coefficient is always a complicated and challenging issue in the automotive engineering. There are different approaches and experimental studies to try to find the solution of this problem. An excellent review can be found in [6].

There are already some interesting solutions on the topic of this problem. For example, the physical sensor-oriented techniques measures the road surface friction conditions directly or indirectly by using special sensors, such as tire noise sensor, optical sensor, tire strain and pressure sensors. In [7, 8], the road surface condition is recognized on the basis of image processing techniques and the image is taken using a carmounted camera. This method is effective at measuring the road surface condition. However, this method is extremely influenced by the direction and intensity of light and the clarity of the image is often reduced. Eichhorn used acoustic sensors near the tire to detect the road condition from tire-road sound [9]. These solutions may perform well, but are quite expensive. They also have the principal and basic limitations due to the physically detected conditions.

Another available solution which is utilized in the present work for this identification purpose, is the well-known slip-based approach, which uses the tire/road friction force models based on the wheel slip [10]. Real-time and robust process in this case, have recently become more important. An excellent review can be found in [4]. In [11] a sliding mode control is used together with a Grey predictor to estimate the road conditions. Such approaches are computationally demanding and difficult to implement in real-time and also have a slow convergence.

In the present work, the friction coefficient is modeled with semi-empirical formulas, which generate the steady-state wheels behavior. One of the widely-used models is The Burckhardt Model [12], which is easy to linearize to apply recursive least squares (RLS) estimator and allows a good correlation to be obtained with experimental results. Tanelli et al. [13] have proposed a new real-time identification approach for the wheel slip corresponding to the peak of the tire-road friction curve using linearized form of simple Burckhardt model, based on the widely-used recursive least squares (RLS) methods. In addition to this important approach, maximum likelihood estimation method using Non-linear Burckhardt model however, was not fast, accurate and recursive, but also has been proposed. De Castro et al. [14] have improved this approach by proposing more accurate linear parametrization (LP) for Burckhardt model and offering the constrained version of RLS for the estimation case. Although this approach solves the problem of identification, it also doesn't have enough fitting with experimental data due to tire changes and has a linearization issue and its own errors. In order to obtain more reliable detections, some other prediction approaches have been proposed and the results have been presented for different road surfaces [15–17]. Most of these methods have employed simple vehicle dynamics because of estimation accuracy problem on a more complex vehicle dynamic

model.

Based on the above discussion, it can be said that limited works have been reported for a real-time and robust detection of tire/road conditions. Therefore, this work is focused on implementing a computationally efficient algorithm for on-line identification of surface conditions for different tire types and road surface conditions during braking. First, the system is modeled and a new efficient real-time estimation approach is presented [18]. Furthermore in order to consider the friction coefficient dependence on velocity and also to involve more properties of real friction behavior such as tire situation, LuGre dynamic friction model, is used together with Burckhardt Model, which proposing an improved version of the algorithm, which accurately fits curves and allows the adaptation to different road conditions [19]. There is also a discussion about the possibility of the presented approach to estimate the road conditions, see also [20].

In the proposed method, the LuGre model is a static one obtained from the LuGre distributed model. Then a new LuGre model-based nonlinear least squares (NLLS) parameter estimation algorithm (based on recursive nonlinear optimization of the curve fitting errors) using the proposed static form of the LuGre to obtain its parameters is presented. Optimization problem is solved by using an interior Trust-Region method. This method is robust and gives faster convergence rates by proper initialization of the vector function [21–23]. In order to initialize, the RLS identification is employed to identify the linear parametrization (LP) form of Burckhardt model in real time. The identified parameters provide through a fuzzy system the initial values for the LuGre model and so the fuzzy rule base plays a key role as converter between two different structures. The advantage of the proposed approach is that, although it uses a nonlinear identification system, it still results relatively good as concerns convergence rate if it is compared with the results of linear approach. This also involves more properties of real friction behavior especially due to having nonlinear scheme. As was said, the presented approach has the advantage of computational simplicity and also the parameters can be obtained simultaneously and recursively not only for the linear estimation, but also for the general nonlinear system.

This work also presents the vehicle dynamics and tire-surface interaction model following which the method to identify surface characteristics. This mixed identification strategy utilizes both presented ways using Takagi-Sugeno fuzzy method to convert Burckhardt road type characteristics to LuGre road-tire parameters. The organization of the remaininig part of this paper is as follows. In Section 2 the four wheel vehicle model, the Burckhardt and LuGre dynamic tire models, are presented, respectively. Different simulation results and analysis based on a full-vehicle model and experimental data, are discussed in Section 4. Conclusive remarks are presented in Section 5.

2. System description

A simple but effective four-wheel vehicle considering vehicle/tire/road dynamics is described in this section [4, 24].The dynamic equations are the result of application of Newton-Euler law for the vehicle and wheel.

The vehicle dynamic is given by summing the total forces applied to the vehicle with braking operation. Ignoring the road gradient [25] and wind speed it is represented as

$$\dot{v}_v = \frac{-1}{M_v} \left[\sum F_{xi} + B_v v_v + D_a v_v^2 \right] \tag{1}$$
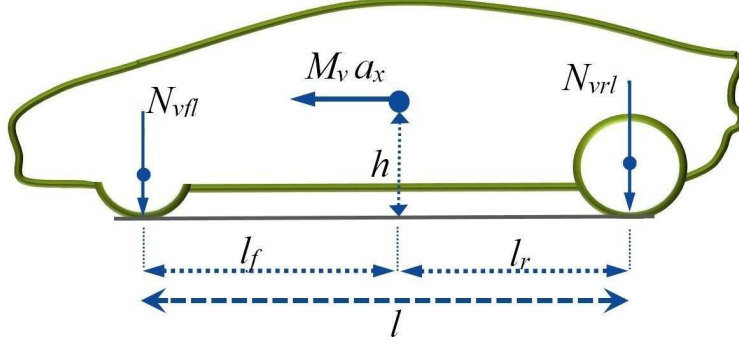
Figure 1. Vehicle dynamics scheme during deceleration.

where $v_v[m/s]$ is the longitudinal velocity of the vehicle; $M_v[kg]$ is the mass of the vehicle at center of gravity (CG); $F_{xi}[N]$ denotes the tire/road friction force for the wheel $\{i = fl, fr, rl, rr\}$, $(f = front/r = rear, l = left/r = right)$; B_v is the vehicle viscous friction; D_a is the aerodynamic drag force coefficient so that

$$D_a = 0.5\zeta C_d A \tag{2}$$

with $\zeta[kg/m^3]$ being the air density, C_d the aerodynamic drag coefficient, and $A[m^2]$ the frontal area of the vehicle. The tire/road friction force for the ith wheel, is given by

$$F_{xi} = \mu(\lambda)F_{Ni}, \quad \{i = fl, fr, rl, rr\} \tag{3}$$

where the coefficient of friction μ is a function of the slip λ; and $F_{Ni}[N]$ denotes the vertical wheel reaction force applied to the wheel.

As it has been previously discussed by the authors [26, 27], the weight is transferred between the wheels during different car accelerations, thus F_{Ni} varies at the different wheels. The model force, F_{Ni} for the four wheel forces can be expressed as follows

$$F_{Ni} = \begin{cases} \frac{M_v(l_r g + h a_x)}{l}\left(\frac{1}{2} + \frac{h a_y}{d_f g}\right) & i = fl \\ \frac{M_v(l_r g + h a_x)}{l}\left(\frac{1}{2} - \frac{h a_y}{d_f g}\right) & i = fr \\ \frac{M_v(l_f g - h a_x)}{l}\left(\frac{1}{2} + \frac{h a_y}{d_r g}\right) & i = rl \\ \frac{M_v(l_f g - h a_x)}{l}\left(\frac{1}{2} - \frac{h a_y}{d_r g}\right) & i = rr \end{cases} \tag{4}$$

where a_x and a_y (rightwards positive) are the longitudinal and lateral acceleration of CG, respectively, h denotes the height of CG, l_r, l_f are distance from CG to rear and front axles with $l = l_r + l_f$ as the wheelbase of the vehicle, see Fig. 1 and 2, and d_f, d_r, are the transversal distances between wheels on the front and rear axles, respectively [28].

The ith wheel dynamic by summing the rotational torque yields to

$$\dot{\omega}_{wi} = \frac{1}{J_w}\left[-T_{bi}sign(\omega_{wi}) + R_w F_{xi} + T_e\right], \tag{5}$$
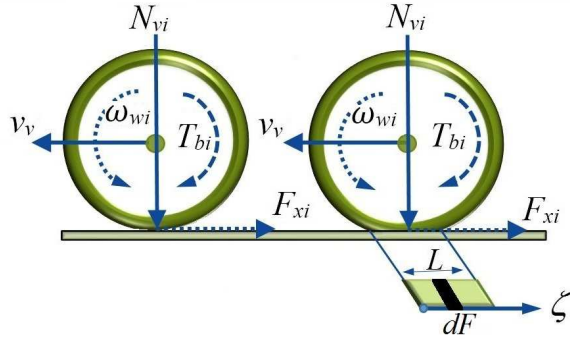
$$\{i = fl, fr, rl, rr\}$$

4

Figure 2. Vehicle wheel with lumped friction (left), and distributed friction (right).

where $\omega_{wi}[rad/s]$ is the angular velocity of the ith wheel, $J_w[kg.m^2]$ denotes the rotational inertia of the wheel, $T_{bi}[N.m]$ is the braking torque on the ith wheel, $R_w[m]$ is the radius of the wheel, and $T_e[N.m]$ is main shaft torque on the wheel [29]. Longitudinal Slip λ is defined as the difference between vehicle actual longitudinal velocity and wheel circumferential velocity, i.e.

$$\lambda = \frac{v_v - v_w}{max\left\{v_v, v_w\right\}} \tag{6}$$

with $v_w = R_w\omega_w$. According to the adopted definition $\lambda \in [-1, 1]$, and λ is negative in traction and positive during braking.

As experimentally investigated in [30], the friction coefficient can be modeled with semi-empirical formulas, which generate the steady-state wheels behavior. One of the most widely-used models is the Burckhardt Model, which is easy to linearize for applying recursive least squares (RLS) identification method and allows a good correlation to be obtained with experimental results. On the other hand, as shown in Fig. 3, with increasing the vehicle speed, the friction coefficient for a given road condition reduces, which is a fact that is generally not considered in these formulas [5].

Therefore in order to consider the friction coefficient dependence on velocity and also to involve more properties of real friction behavior such as tire situation, LuGre dynamic friction model [31], is chosen in addition to the Burckhardt Model, which is accurately fitted curves that allows the adaptation to different road conditions while this last model is identifying the road-tire friction parameters [32].

The Burckhardt friction model can be represented by the following equations:

$$\mu(\lambda; c_\theta) = c_1(1 - e^{-\lambda c_2}) - \lambda c_3 \tag{7}$$

where the Burckhardt elements vector is $c_\theta = [c_1 \quad c_2 \quad c_3]^T$; c_1, c_2 give the maximum value of friction curve and the friction curve shape, respectively; c_3 represents the friction curve difference between the maximum value and the value at $\lambda = 1$.

Also the lumped LuGre model, as proposed in [5, 31] is given as,

$$
\begin{aligned}
\dot{z} &= v_r - \theta\frac{\sigma_0|v_r|}{g(v_r)}z \\
F_x &= (\sigma_0 z + \sigma_1\dot{z} + \sigma_2 v_r)N_v \\
g(v_r) &= \mu_c + (\mu_s - \mu_c)e^{-\left|\frac{v_r}{v_0}\right|^{1/2}}
\end{aligned} \tag{8}
$$

5

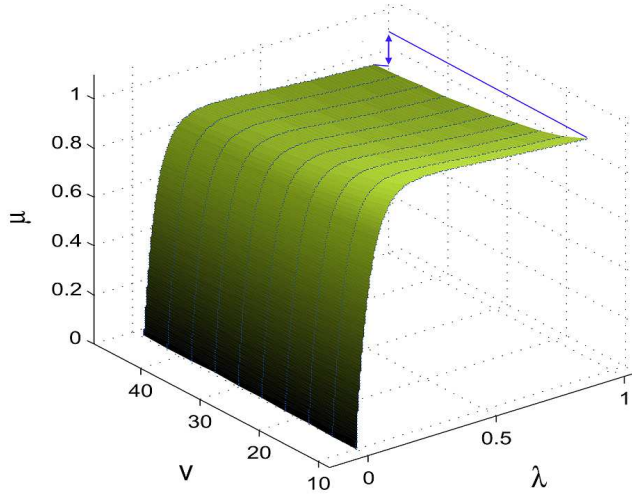Figure 3. Three-dimensional plots of the corresponding (μ, λ, v) for LuGre model.

θ is the road condition parameter that capturing the changes in the road characteristics, σ_0 is the rubber longitudinal lumped stiffness, σ_1 is the rubber longitudinal lumped damping, σ_2 is the viscous relative damping, μ_c is the normalized Coulomb friction, μ_s is the normalized static friction, v_0 is the Stribeck relative velocity, z is the internal friction state, and v_r is a relative velocity defined as $v_r = (v_v - R_w \omega_w)$. A three- dimensional plot of the corresponding (μ, λ, v_v) for this model is shown in Fig. 3.

Assuming that the wheel radius (R_w) remains constant during braking, according to the λ definition in equation (6), a derivation of the longitudinal ith wheel slip dynamics is obtained by taking the derivative of the longitudinal slip, as shown below.

$$\dot{\lambda}_i = -\frac{R_w}{v_v}\dot{\omega}_{wi} + \frac{\omega_{wi} R_w}{v_v^2}\dot{v}_w \tag{9}$$

Ignoring main shaft torque, substituting $R_w \omega_{wi} = v_v(1-\lambda)$, the vehicle rotational and dynamic model in equations (4), (5) and expression of F_{xi} in equation (3) into the above equation, yields to

$$\begin{aligned}
\dot{\lambda}_i = &-\frac{1}{v_v}\left[\frac{(1-\lambda_i)\sum\limits_{i} F_{Ni}}{M_v} + \frac{R_w{}^2}{J_w}F_{Ni}\right]\mu(\lambda_i)\\
&+\frac{R_w}{J_w v_v}T_{bi}sign(\omega_{wi}) - \frac{1-\lambda}{M_v}(D_a v_v + B_v),\\
&\{i = fl, fr, rl, rr\}
\end{aligned} \tag{10}$$

6

3. IDENTIFICATION OF TIRE-ROAD FRICTION CHARACTERISTICS

According to the equation (4), summing the total vertical wheel reaction forces applied to the vehicle yields

$$\sum_i F_{Ni} = M_v g \tag{11}$$

In order to obtain $\mu(\lambda_i) = \mu(\omega_{wi}, T_{bi}, v_v, \lambda_i)$, the result of the Equation (11) must be applied to the inverted form of Equation (10), and so it can be written as follows

$$\mu(\lambda_i) = \frac{\frac{R_w}{J_w v_v} T_{bi} sign(\omega_{wi}) - \dot{\lambda}_i - \frac{1-\lambda_i}{M_v}(D_a v_v + B_v)}{\frac{1}{v_v}\left[(1-\lambda_i)g + \frac{R_w^2}{J_w}F_{Ni}\right]} \tag{12}$$

$$\{i = fl, fr, rl, rr\}$$

According to equation (12), in order to estimate (μ), the signals $\omega_{wi}, v_v, \lambda_i$ and T_{bi} are required at each wheel $\{i = fl, fr, rl, rr\}$ in real time. Angular velocity of each wheel (ω_{wi}) can be measured easily from the rotary encoders. The modern electromechanical brakes (EMB) utilize numerous sensors installed on the EMB caliper and so the brake torque can be directly measured using the measurements of the brake clamping force. Hence the braking torque of ith wheel $(T_{bi}(t))$ is calculated by $T_{bi} = k_B F_{bi}$, where the clamping force $F_b(t)$ is the output of the servo-controlled EMB. In this study, the electromechanical brake will be considered, and its closed-loop dynamics is described as a first-order system transfer function with delay as follows [4]

$$G_{caliper} = \frac{w_{rot}}{s + w_{rot}}e^{-s\tau_M} \tag{13}$$

Remark 1   Although the braking torque measurement was solved by $T_{bi} = k_B F_{bi}$ [4], it is important to note that the friction parameter between the brake pads and the brake disk $k_B \in \Re^+$ is not constant and high temperature rise can even result in friction coefficient variation between brake pads and brake disk in non-negligible range. For instance in [33] it is explained how the temperature affects the friction coefficient on the brake torque characteristic.

Therefore braking torque can be presumed to be measurable in real-time. When $v_v \neq v_w$, the longitudinal speed v_v is principally not measurable and needs to be estimated (see [34]). Hence the parameter λ_i can easily calculated from $\lambda_i = (v_v - R_w \omega_{wi})/v_v$. Finally $\mu(\lambda_i)$ can be obviously obtained by substituting $v_v = R_w \omega_{wi}/(1 - \lambda_i)$ and equations (4) into the equation (12) as shown

$$\mu(\lambda_i; i) = \frac{\frac{T_{bi}(t)sign(\omega_{wi}(t))}{J_w} - \Phi_1(t)\dot{\lambda}_i(t) - \frac{\Phi_2(t)}{M_v}}{\frac{g\omega_{wi}(t)}{R_w \Phi_1(t)} + \frac{R_w M_v}{2J_w l}\Xi_{1i}(t)(1 + \Xi_{2i}(t))}, \tag{14}$$

$$\{i = fl, fr, rl, rr\}$$

$$\begin{pmatrix} \Xi_{1fl}(t) \\ \Xi_{1fr}(t) \\ \Xi_{1rl}(t) \\ \Xi_{1rr}(t) \end{pmatrix} = \begin{pmatrix} 1 & 0 \\ 1 & 0 \\ 0 & 1 \\ 0 & 1 \end{pmatrix} \begin{pmatrix} l_r g + h a_x(t) \\ l_f g - h a_x(t) \end{pmatrix}$$

$$\begin{pmatrix} \Xi_{2fl}(t) \\ \Xi_{2fr}(t) \\ \Xi_{2rl}(t) \\ \Xi_{2rr}(t) \\ \Phi_1(t) \\ \Phi_2(t) \end{pmatrix} = diag(1,1,1,1,\omega_{wi}(t),\omega_{wi}(t)) \begin{pmatrix} 1 + \frac{2ha_y(t)}{d_f g} \\ 1 - \frac{2ha_y(t)}{d_f g} \\ 1 + \frac{2ha_y(t)}{d_r g} \\ 1 - \frac{2ha_y(t)}{d_r g} \\ \frac{1}{1-\lambda_i(t)} \\ D_a R_w \Phi_1(t) + B_v \end{pmatrix}$$

As seen from the friction coefficient estimation in equation (14) and according to the equation $\mu = F_{xi}/F_{Ni}$, the vertical wheel reaction force plays an important role in determining the maximum force the tire can generate. For the same road surface and tire type, a larger vertical force, results in a larger longitudinal force. According to the equation (14) the mass of the vehicle is the main portion of the normal force, and the vehicle longitudinal acceleration forces acting on the vehicle during longitudinal maneuvers redistribute the vertical forces between the tires.

3.1.   *Setting the initial conditions*

In equation (7), the Burckhardt model is nonlinear due to the exponential term in c_2 . If the linear form of μ Burckhardt model is determined, its unknown parameters will be estimated by linear least-squares methods. Therefore the problem is finding an optimal linear parameterization (LP) for the single nonlinear term $f(\lambda, c_2) = e^{-c_2 \lambda}$ with the approximating domain $[0, \bar{\lambda}] \times D$,

$$\begin{aligned} \hat{f}(\lambda, w, \beta) &= [g_1(\lambda, w), \cdots, g_n(\lambda, w)]\beta \\ &= G(\lambda, w)^T \beta \end{aligned} \tag{15}$$

where the principal functions for LP are

(1) Exponential: $G_E(\lambda, w) = \begin{bmatrix} e^{w_1 \lambda} & e^{w_2 \lambda} , \cdots, & e^{w_m \lambda} \end{bmatrix}^T$
(2) Logistic sigmoid:

$$G_E(\lambda, w) = \begin{bmatrix} \frac{1}{1+e^{-w_1 \lambda - w_2}} , \cdots, & \frac{1}{1+e^{-w_{m-1} \lambda - w_m}} \end{bmatrix}^T$$

with $w = [w_1 \ w_2 , \cdots, w_m] \in \Re^m$

Even though both functions can produce a reasonable LP results, the number of the parameters of exponential function is less than logistic sigmoid.

Remark 2   In [35, 36] the different values of optimum w were used in exponential function to decrease the approximation error and to give the good LP with the number of the basis $n = 4$. On the other hand, reducing the number of the exponential functions, can speed up the estimation. Therefore, in this paper, the exponential functions were implemented for the real-time estimation with the optimum w as $G(\lambda) = [e^{-4.99\lambda} \ e^{-18.43\lambda} \ e^{-65.62\lambda}]^T$

[37]. This approximation reduces the number of exponential functions to $n = 3$ and it is as accurate as the complex LP forms presented in [35].

As a result the LP is as follows

$$\hat{\mu}(\lambda; t) = a_1 - a_2\lambda + a_3 e^{-4.99\lambda} + a_4 e^{-18.43\lambda} + a_5 e^{-65.62\lambda} \tag{16}$$

It can be recognized as linear regression

$$\begin{aligned} \hat{\mu}(\lambda; t) &= \phi(\lambda)^T a \\ \phi(\lambda; t) &= \begin{bmatrix} 1 & -\lambda & e^{-4.99\lambda} & e^{-18.43\lambda} & e^{-65.62\lambda} \end{bmatrix}^T \\ a &= [a_1 \ a_2 \ , \cdots , a_5]^T \end{aligned} \tag{17}$$

where a_1 and a_2 are equal to c_1 and c_3 in Burckhardt model (7). Therefore, the recursive least squares (RLS) algorithm [38], can be used to update the unknown parameter vector of a iteratively, using the past input-output data contained within the measured regressor vector $\phi(t)$.

Algorithm 1 RLS identification algorithm for this problem

1: **for** $k \leftarrow 0, 1, \dots$ **do** Measure and calculate μ_k and ϕ_k.
2:     calculate the estimation error, $e_k = \mu_k - \phi_k^T c_{k-1}$
3:     Calculate K_k and P_k as

$$K_k = \frac{P_k \phi_k}{\zeta + \phi_k^T P_k \dot{\phi}_k}; \ P_k = \frac{1}{\zeta}\left[P_{k-1} - \frac{P_{k-1}\phi_k \phi_k^T P_k}{\zeta + \phi_k^T P_k \phi_k} \right]$$

4:     Update the estimated parameter as

$$c_k = c_{k-1} + K_k e_k.$$

5:     $k = k + 1$
6: **end for**

According to the algorithm 1, e_k is the difference between the system actual output at the present sample and the output predicted in previous sample, K_k is the update gain vector and P_k is the covariance matrix. The parameter ζ is called the forgetting factor, which is chosen between $(0.9, 1)$ and adjusts the influence of old data. While the small values of forgetting factor, tracking ability to time-varying parameters improve at the expense of sensitivity to noises; its larger values will provide robustness to the noise but its tracking ability will be poor.

Figure 4. Proposed NLLS algorithm architecture.

The structure of the proposed algorithm is shown in Fig. 4. As shown in this structure, in order to complete the identification steps Burckhardt road type characteristics should be converted to LuGre road-tire parameters. The proposed formulation for this case is an instance of the Takagi-Sugeno (TS) fuzzy system (see Fig. 5).
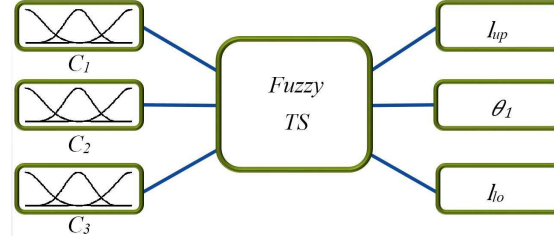

Figure 5. Fuzzy logic based parameter conversion.

Hence the rule base for this model can be written using the set of M rules [39], as follows:

$$R = \left\{ R_{Bklg}^1, \ R_{Bklg}^2, \ , \cdots, R_{Bklg}^M \right\} \tag{18}$$

where the kth rule has the following format:

$R_{Bklg}^k :$ **IF** C_1 is $\tilde{A}_1^k$ OR C_2 is $\tilde{A}_2^k$ OR C_3 is $\tilde{A}_3^k$, **THEN**
θ_{up} is $\tilde{B}_1^k$ AND θ is $\tilde{B}_2^k$ AND θ_{low} is $\tilde{B}_3^k$, $\quad k = 1,..M$
where $\tilde{A}_j^k$ are the classified inputs and $\tilde{B}_j^k$ are fuzzy sets defined by multivariate membership functions using experimental results of Burckhardt and LuGre models [4, 5].

3.2. NLLS estimation approach

LEMMA 1 *For any given road condition and tire types if v, ω are assumed to be constant during each estimation period and conditions of braking case hold, then the following static form can be used to identify LuGre tire-road friction parameters by fitting the model to experimental data, i.e.,*

$$\mu_b(\lambda) = \frac{g(\lambda)}{\theta} \left[1 + \frac{g(\lambda)(\lambda+1)}{\theta \sigma_0 \lambda L} (e^{-\frac{\sigma_0 \lambda L \theta}{g(\lambda)(\lambda+1)}} - 1) \right] + \sigma_2 \lambda v_v \tag{19}$$

10

where

$$g(\lambda) = \mu_c + (\mu_s - \mu_c)e^{-\left|\frac{\lambda_v}{v_0}\right|^{1/2}}$$

Proof. See Appendix A for the derivation of the model. ∎

After collecting N samples of $\lambda_i \in \Re^N$ at the current time, nonlinear least squares (NLLS) approach can be set up to the estimation method. Let $\mu_a \in \Re^N$ to be the vector of friction which is calculated from the equation (14) for different values of λ_i and $\hat{\mu}_b(\lambda_i, \Theta) \in \Re^N$ be the vector of LuGre friction model (19) with unknown parameters and the sample vector of λ_i.

$$f_\epsilon(\Theta) = |\mu_a - \hat{\mu}_b(\lambda_i, \Theta)| \tag{20}$$

Now the LuGre unknown parameters are available by minimizing the estimation error $f_\epsilon(\lambda_i)$ [40]. Iterative methods for nonlinear optimization can be classified into line search methods and trust region methods. Trust region methods are robust and give faster convergence rate for minimizing vector-function with large number of elements. Thus in order to solve subproblem (21) an interior Trust-Region method [21, 22], is utilized in the present work.

$$\text{minimize} \ \ f_\epsilon(\Theta) \ \text{subject to} \ \Theta \in [l_{lo}, l_{up}], \tag{21}$$

Assuming that the first and second derivatives of f_ϵ are all continuous in a neighborhood D_f, the quadratic approximation can be defined by the first two terms of local Taylor expansion of $f_\epsilon(\Theta)$ at Θ , i.e.,

$$f_\epsilon(\Theta + s) \approx f_\epsilon(\Theta) + \underbrace{s^T \nabla f_\epsilon(\Theta_k) + \frac{1}{2} s^T \nabla^2 f_\epsilon(\Theta_k)s}_{\psi_k(s)} \tag{22}$$

which yields to

$$\begin{aligned} &\min_{s \in \Re^N} \ \ s^T g_k + \tfrac{1}{2} s^T H_k s = \psi_k(s) \\ &such \ that \ \ \ \|s\|_2 \leq \Delta_k, \end{aligned} \tag{23}$$

where $g_k = \nabla f_\epsilon(\Theta_k)$ is the gradient at the current iteration, $H_k = \nabla^2 f_\epsilon(\Theta_k)$ is symmetric matrix denoting the Hessian of $f_\epsilon(\Theta)$ and $\Delta_k > 0$ is a trust region radius. The standard form $\psi_k(s)$ is a scalar function which can be easily solved with computational optimization methods [23, 41]. That is to say $\psi_k(s)$ is a model of reduction in f_ϵ within the neighborhood of iterate Θ_k. This suggests that it may be desirable to calculate Trust-Region step s_k which solves subproblem (23). Now Θ_k can be updated by 8.2 (see algorithm 2).

Remark 3   As it is pointed in step 8.3 (algorithm 2) if updating term $\Theta_{k+1} = \Theta_k + s_k$ produces a sufficient reduction in f_ϵ, then Δ_k can be increased; else if it doesn't satisfy the acceptable range of reduction then Δ_k should be decreased.

The convergent solution is achieved after only about 5 iterations. The proposed identification method is summarized in algorithm 2.

Algorithm 2 Trust-Region based recursive identification algorithm for this problem

---

1: Initialisation of the Burckhardt parameter vector
2: **repeat**
3:      Measure $\mu_a \in \Re^N$ and calculate $\lambda_i \in \Re^N$ using (14)
4:      Determine the Burckhardt parameter vector using Algorithm 1 RLS method
5:      Calculate $f_\epsilon(\Theta) = \mu_a - \hat{\mu}_b(\lambda_i, \Theta)$
6:      Obtain $\Theta_1, l_{lo}, l_{up} \in \Re^N$ using fuzzy (18)
7:      Given $\Delta_1 > 0$ let $k = 1$,
8:      **while** (Not converged) **do**
9:          8.1)   Solve subproblem (23) giving s_k
10:         8.2)   Update Θ_k, i.e.

$$\Theta_{k+1} = \begin{cases} \Theta_k & \text{if } \Theta_k + s_k \notin [l_{lo}, l_{up}] \text{ or } f_\epsilon(\Theta_k) \leq f_\epsilon(\Theta_k + s_k) \\ \Theta_k + s_k & \text{otherwise,} \end{cases} \qquad (24)$$

11:         8.3)   Trust region radius update. Set

$$r_k = \left(f_\epsilon(\Theta_k) - f_\epsilon(\Theta_k + s_k) \right) / \psi_k(s_k)$$

$$\Delta_{k+1} \in \begin{cases} [\tau_3 \|s_k\|_2, \ \tau_4 \Delta_k] & \text{if } r_k < \tau_2, \\ [\Delta_k, \ \tau_1 \Delta_k] & \text{otherwise;} \end{cases}$$

12:         8.4)   Update g_k, H_k and $k = k + 1$
13:     **end while**
14:     Update inputs
15: **until** (there are no more input data available)

According to the algorithm 2, the typical values of constants $\tau_i(i = 1, ..., 4)$ in [41], are $\tau_1 = 2$, $\tau_2 = \tau_3 = .25$, $\tau_4 = 0.5$. The following assumption will be made throughout the paper.

ASSUMPTION 1   *Let $f_\epsilon(\Theta_k) : \Re^n \to \Re$ is twice continuously differentiable and bounded below on $\Re^n$. Assume that there exists a bounded convex closed set $\Omega \subset \Re^n$ such that Θ_k are in Ω for all k. Also note that $\nabla^2 f_\epsilon(\Theta_k^*)$ is assumed to be nonsingular where Θ_k^* is a limit point of $\{\Theta_k\}$.*

THEOREM 1   *For the friction model with unknown parameters and algorithm in (8) under assumption (1) if the conditions of algorithm (2) hold, then the asymptotic convergence is guaranteed and the process is completely identifiable.*

Proof. According to the problem conditions assume that $f_\epsilon(\Theta_k) : \Re^n \to \Re$ is twice continuously differentiable and bounded below on $\Re^n$. In order to prove the theorem first is noted that $\nabla^2 f_\epsilon(\Theta_k^*)$ is assumed to be nonsingular where Θ_k^* is a limit point of $\{\Theta_k\}$. Now by the conditional john-reigns lemma [42], it can be shown that $\nabla^2 f_\epsilon(\Theta_k^*)$ is positive definite. Choose $\delta > 0$ so that $\nabla^2 f_\epsilon(\Theta_k^*)$ is positive definite for $\|\Theta - \Theta^*\| \leq \delta$. Hence there is an $\epsilon_1 > 0$ with $\|\Theta_k - \Theta^*\| \leq \delta$ such that

$$\epsilon_1 \|s_k\| \leq \|\nabla f_\epsilon(\Theta_k)\|. \tag{25}$$

By referring to [43], it can be proved that $\{\nabla f_\epsilon(\Theta_k)\}$ converges to zero, and thus there is an index $k_1 \geq 0$ such that

$$\|\nabla f_\epsilon(\Theta_k)\| \leq \frac{1}{2}\epsilon_1\delta, \quad k \geq k_1. \tag{26}$$

Since $\Theta_{k+1} = \Theta_k + s_k$ using (25) and (26), for $k \geq k_1$ implies that $\|\Theta_{k+1} - \Theta^*\| \leq \delta$, if and only if $\|\Theta_k - \Theta^*\| \leq \delta/2$. Now, since $\nabla^2 f_\epsilon(\Theta_k^*)$ is positive definite, since $\nabla f_\epsilon(\Theta_k^*) = 0$, and since Θ_k^* is a limit point of $\{\Theta_k\}$, it is easy to show that there is an index $k_2 \geq k_1$ with $\|\Theta_{k_2} - \Theta^*\| \leq \delta/2$, it follows that $f_\epsilon(\Theta) \leq f_\epsilon(\Theta_{k_2}), \quad \|\Theta - \Theta^*\| \leq \delta \Rightarrow \|\Theta - \Theta^*\| \leq \delta/2$ which yields for $k \geq k_2$,

$$\underbrace{\|\Theta_k - \Theta^*\| \leq \delta}_{\delta\ chosen} \Rightarrow \|\Theta_k - \Theta^*\| \leq \delta/2. \tag{27}$$

Hence $\delta = 0$, is chosen to satisfy (27) and leads to $\{\Theta_k\} \to \Theta^*$. Since $f_\epsilon(\Theta^*) = |\mu_a - \hat{\mu}_b(\lambda_i, \Theta^*)| = 0$ the parameter estimation error given by above equation consistently converges to zero. Thus the theorem 2 is proven. ∎

4. SIMULATION RESULTS

The estimation of tire/road friction conditions is one of the applications that can benefit most from the presented NLLS identification algorithm. To highlight this aspect, this section presents simulation results to validate the proposed non-linear model in estimating the longitudinal friction curve and other friction characteristics with the presented NLLS method. The simulation is performed under two different conditions (fixed-μ and mixed-μ). Since the friction parameters results of vehicle different wheels do not show considerable differences, average value of the four wheels is illustrated in the figures.

Since the estimation needs the stable value of the slip under varying friction conditions, the slip control method presented in [44] has been used for this case (see Fig. 6). In order to have more accurate identification results, the rubber stiffness σ_0 is assumed to be available, thus $\Theta = \theta$. The sampling time of the simulation was set to 5ms and In order to consider more realistic settings, the prediction has been done on noisy simulation data. Zero mean white noises have been added to the wheel speed with $\sigma_\omega^2 = .01\,rad^2/s^2$, to the braking torque with $\sigma_{Tb}^2 = 10\,N^2m^2$, and to the rubber stiffness with $\sigma_{\sigma_0}^2 = 15\,1/m^2$, due to the measurement noise by wheel encoder, EM-brakes and rubber stiffness uncertainty,
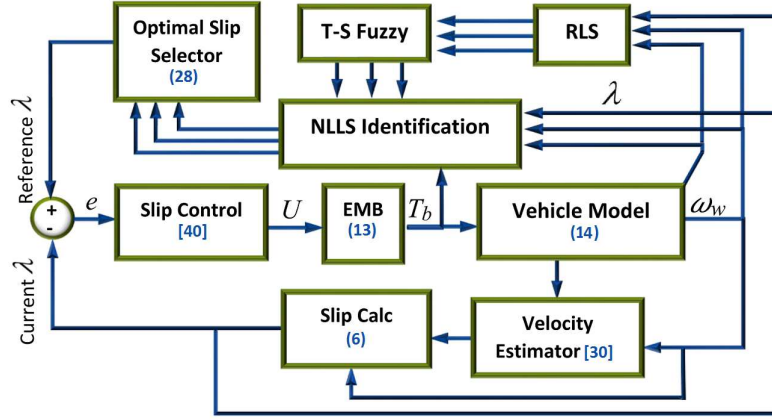
Figure 6. Implementation of the proposed NLLS.

respectively. In the case of v_v, the variances have been included in the velocity by the range of $\sigma_v^2 \in [.15\ .3]\ m^2/s^2$ to indicate estimation errors on road with different roughness. Hence the longitudinal velocity estimation results of [34] have been used in this case. The main parameter values for the vehicle are listed in Table 1.

Table 1. Vehicle nominal parameters [4, 5]

Symbol	Value	Symbol	Value
R_w	$.3\,[m]$	L	$.2\,[m]$
J_w	$1\,[kg.m^2]$	μ_c	$.8$
l_f	$1.3\,[m]$	μ_s	$1.55\,[m]$
l_r	$1.4\,[m]$	σ_0	$181.54\,[1/m]$
d_f, d_r	$.9\,[m]$	σ_1	$4.94\,[s/m]$
h	$.5\,[m]$	σ_2	$.0018\,[s/m]$
M_v	$900\,[kg]$	v_0	$6.57\,[m/s]$
ω_{rot}	$70\,[rad/s]$	τ_M	$10\,[ms]$

4.1. *Constant road/tire friction estimation*

In order to benchmark the results, the first task is to compare the identification methods for the constant friction conditions. Two different driving scenarios are considered during braking for this case, where the desired vehicle longitudinal speed is changed from 25 m/s ($90km/h$) to 16 m/s ($56\ km/h$) on dry asphalt during braking (see Fig. 8) and deceleration/braking from 25 to 23 m/s on snow (Fig. 7), respectively.

Table 2. LuGre/Burckhardt curve fitting results in $v = 25m/s$

θ	1	1.5	2	2.5	3	4	5
c_1	.962	.681	.528	.434	.369	.285	.234
c_2	19.51	28.12	36.79	45.56	54.42	72.48	91
c_3	.0891	.0874	.0801	.0724	.0660	.0560	.0401

Both Burckhardt based identification [3] and proposed identification results have been illustrated for these scenarios. Figs. 8 and 7 clearly show that the combined NLLS method
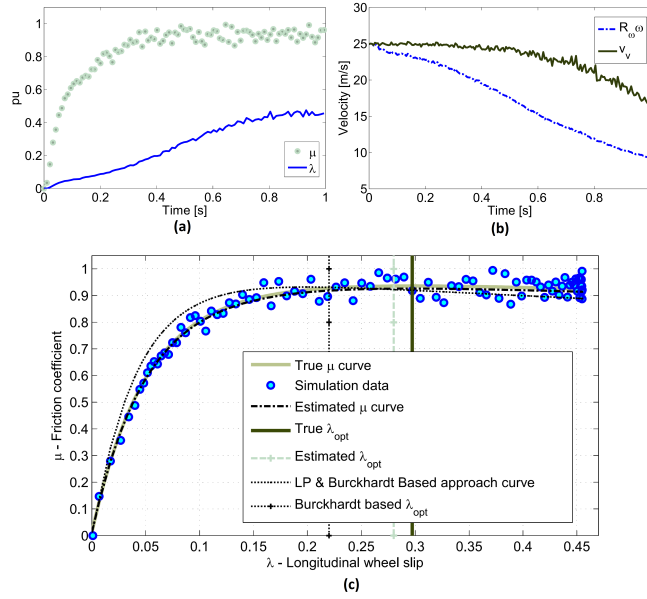
Figure 7. Friction parameters identification results on dry asphalt: (a) wheel slip and friction coefficient, (b) vehicle angular and longitudinal velocities, (c) curve fitting results.
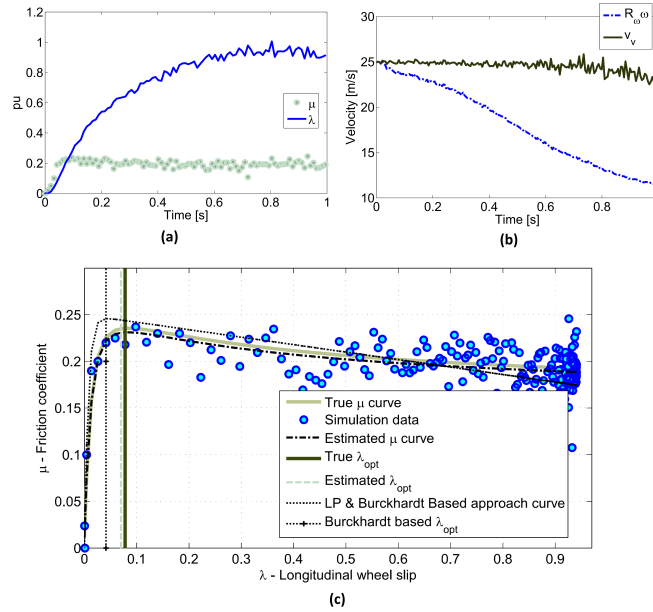

Figure 8. Friction parameters identification results on hard-packed snow: (a) wheel slip and friction coefficient, (b) vehicle angular and longitudinal velocities, (c) curve fitting results.

using both Burckhardt and LuGre models gives better results for the different surfaces. This can also be justified by noting that, combined NLLS method considers more realistic features, such as changes of tire friction characteristics and vehicle longitudinal velocity. Curve fitting based equalization of LuGre and Burckhardt friction models results, using the experimental results of [5], where the desired vehicle longitudinal speed is 25 m/s are listed in table 2.

In order to evaluate the performance of the proposed algorithm more objectively, it is reimplemented in Matlab/Carsim environment. CarSim is a commercial software package
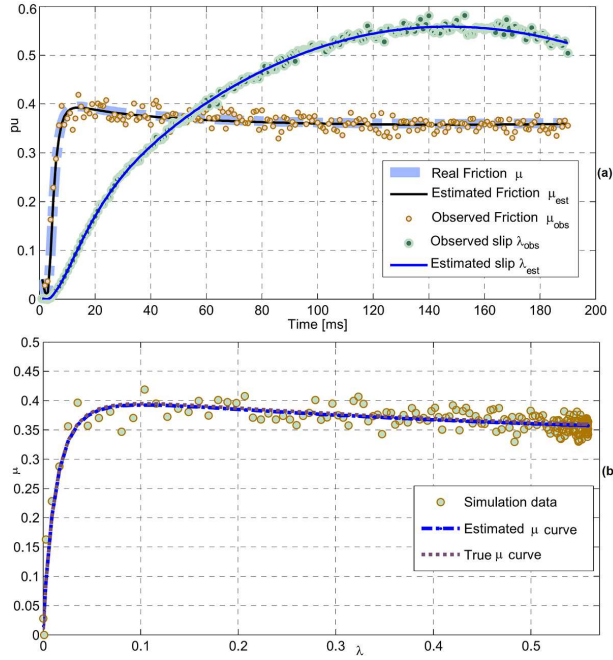
Figure 9. Friction parameters identification results on 40% slippery surface: (a) wheel slip and friction coefficient, (b) curve fitting results.

for simulating and analyzing the behavior of vehicles in response to steering, braking, and acceleration inputs. The simulation is performed under three different road conditions (40% , 55% and 70% slippery surfaces).
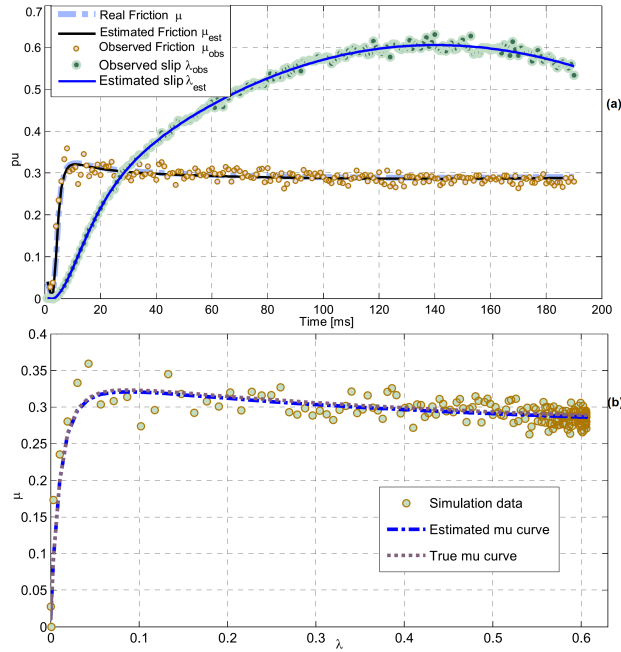

Figure 10. Friction parameters identification results on 55% slippery surface: (a) wheel slip and friction coefficient, (b) curve fitting results.

The values listed in table 1 are also considered for this simulation and vehicle model (see Fig. 6) is re-evaluated as Carsim output. The results shows the proximity between

Simulink and Carsim outputs as well as accurate estimation results for the proposed algorithm.
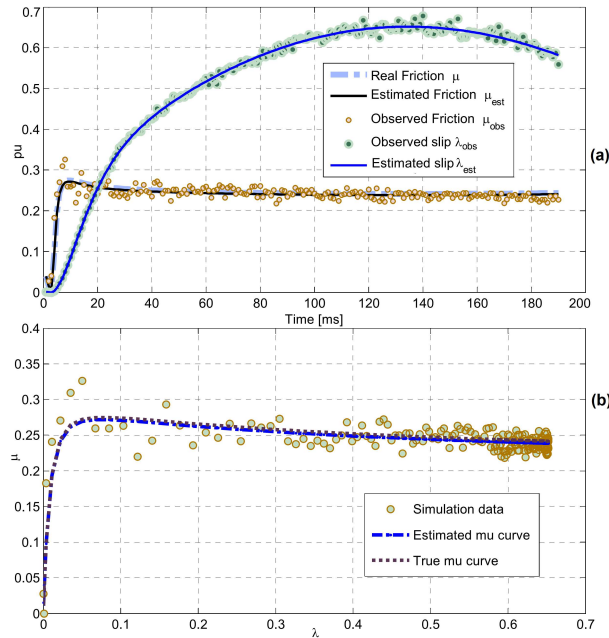

Figure 11. Friction parameters identification results on 70% slippery surface: (a) wheel slip and friction coefficient, (b) curve fitting results.

In the following, the algorithm is also validated using data from experiments. The experimental data have been collected during tire testing experiments on road conducted using a trailer able to impose slip conditions to the tire during a braking maneuver and to measure vertical and longitudinal forces. They have been acquired with a sampling frequency of 100 Hz. According to the results in Figs. 12 and 13, the effectiveness of the estimation of frictional behavior in real experiments shows the same accuracy was seen in simulation results.
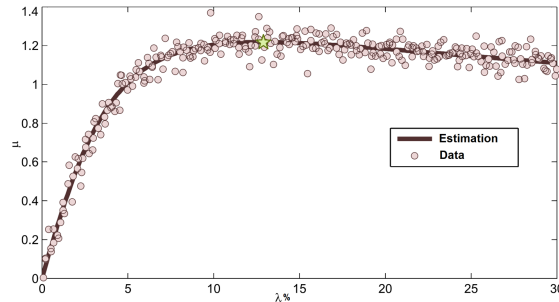

Figure 12. curve fitting experimental results of frictional characteristics for dry asphalt

As it is clear in the Figs. 12 and 13, the maximum point of the estimated friction, which also corresponds to the optimal slip value, is indicated by a star symbol. The tests have been conducted on the same surface in two different conditions (dry and wet) using two identical tyres. By computing the estimated friction maximum point for both dry ($\hat{\mu}_{max}^{dry} = 1.2180$) and wet conditions ($\hat{\mu}_{max}^{wet} = 1.0979$) and comparing them with the relative real values ($\mu_{max}^{wet} = 1.0983$, $\mu_{max}^{dry} = 1.2181$), it is observed that estimation results
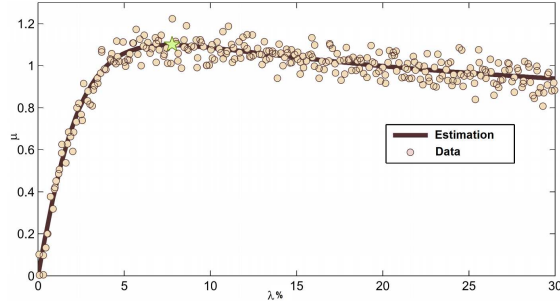
17

Figure 13. curve fitting experimental results of frictional characteristics for wet asphalt

are very accurate. In this case, the optimal values of the slip $\hat{\lambda}_{i_{opt}}$ can be obtained by the estimated friction maximum point.

$$\hat{\lambda}_{i_{opt}} = \arg \max_{\lambda} \ \{\hat{\mu}_b(\lambda_i, v_v, \Theta)\} \tag{28}$$

thus gives $\hat{\lambda}_{opt}^{wet} = 7.35\%$ and $\hat{\lambda}_{opt}^{dry} = 12.65\%$. Real values for the optimal slip are $\lambda_{opt}^{wet} = 7.60\%$ and $\lambda_{opt}^{dry} = 12.81\%$, this means the error rates are $\epsilon_{\lambda}^{wet}\% = 3.289\%$ and $\epsilon_{\lambda}^{dry}\% = 1.249\%$ respectively. Therefore the estimation shows a very good agreement with experimental data.

4.2. *road/tire friction estimation in variable conditions*

In order to validate the effectiveness of proposed friction estimator, a road with variable conditions is simulated. Hence, the remaining work is passed on to the variable tire/road monitoring.

Fig. 14 shows the result of road condition parameter estimation θ. The real θ value first changes from 1 to 3 and then to 2 where the desired vehicle longitudinal speed is changed from 25 m/s to 18 m/s during braking.
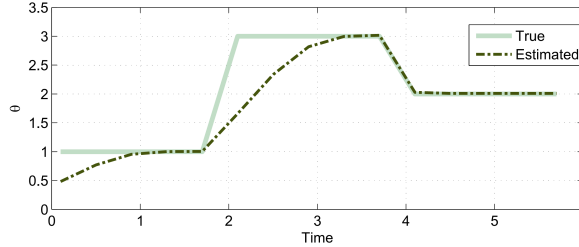

Figure 14. LuGre θ estimation on time-varying road friction condition.

The optimal value of the slip $\hat{\lambda}_{i_{opt}}$ is also obtained by equation (28) and thus the results of peak friction coefficient and its own slip value can be computed (see Fig. 15).

Fig. 16 shows the friction forces between road surface and the vehicle tires during the provided variable friction surfaces computed by the friction coefficient values using equations (4) and (14) which can be helpful for control of vehicle suspension and wheels disturbance estimation [45, 46]. Time history of normalized road-tire friction coefficient estimation error is illustrated in Fig. 17.
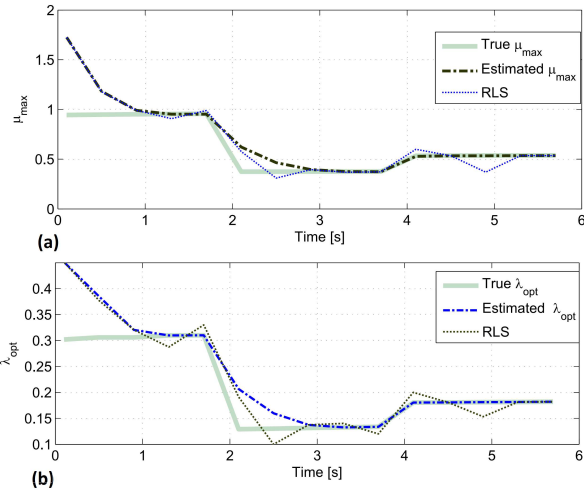
18

Figure 15. $\hat{\lambda}_{i_{opt}}$ and $\hat{\mu}_{max}$ estimation results on time-varying road friction condition.
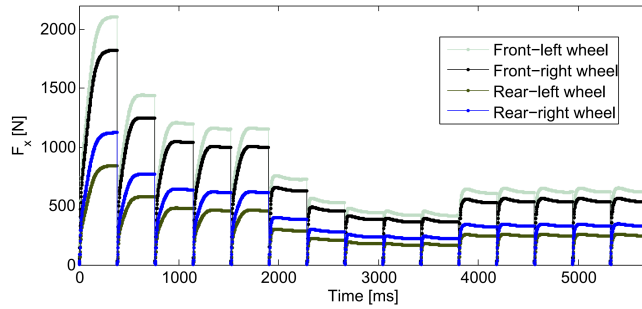

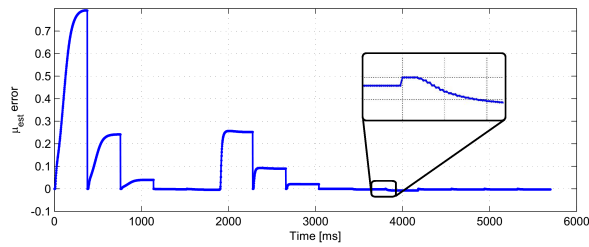Figure 16. Time history of tire-road friction force estimation on time-varying road friction condition.

Figure 17. Time history of normalized road-tire friction coefficient estimation error on time-varying road friction condition.

As shown in Fig. 15, it is indicated that both presented NLLS approach and RLS friction estimator are available for the quick-changes of the road condition and have a good convergence rate. However, with respect to the RLS method [35], from the above results, it can be observed that the NLLS estimated values has a better fit to the real data. This also can be justified by the fact that although the RLS is fast, it assumes multiple linear regression model and has linearization error in this case. NLLS approach doesn't need to approximate the nonlinear models and is more robust to noise.

19

5. Conclusions

In this work an on-line algorithm for the estimation of road surface friction conditions considering various tire friction conditions and different vehicle speeds has been presented. In order to initialize and have a faster algorithm, the parameters of Burckhardt LP form have been identified using RLS and then converted to the LuGre parameters by using the fuzzy rules. The LuGre model is a static one obtained by the LuGre distributed model. A new LuGre model-based NLLS parameter estimation algorithm has been presented based on recursive nonlinear optimization of the curve fitting errors. The convergence of NLLS method has been proved and also the total algorithm performance has been tested when it is used in different time-varying and constant road profiles. The effectiveness of proposed algorithm is demonstrated through simulation as well as experimental results and thus the proposed longitudinal road/tire frictional condition estimation is valuable for advanced vehicle control and autonomous vehicle systems. Although, this estimator used normal vehicle sensors, it still brought relatively good results when compared with the values obtained from the real data. Future work will be devoted to applying full extensions of the estimation to this test vehicle in real-time.

Disclosure

Part of this work [19] was selected for the Best Paper Award at the First International Conference of IFToMM, University of Padova, Vicenza, Italy 2016, which was awarded by the International Federation for the Promotion of Mechanism and Machine Science.

References

[1] Albinsson A, Bruzelius F, Jacobson B, Fredriksson J. Design of tyre force excitation for tyre–road friction estimation. Vehicle System Dynamics. 2017;55(2):208–230.
[2] Chen L, Bian M, Luo Y, Qin Z, Li K. Tire–road friction coefficient estimation based on the resonance frequency of in-wheel motor drive system. Vehicle System Dynamics. 2016;54(1):1–19.
[3] Bhandari R, Patil S, Singh RK. Surface prediction and control algorithms for anti-lock brake system. Transportation research part C: emerging technologies. 2012;21(1):181–195.
[4] Savaresi SM, Tanelli M. Active braking control systems design for vehicles. Springer Science & Business Media; 2010.
[5] Canudas-de Wit C, Tsiotras P, Velenis E, Basset M, Gissinger G. Dynamic friction models for road/tire longitudinal interaction. Vehicle System Dynamics. 2003;39(3):189–226.
[6] Rajamani R, Phanomchoeng G, Piyabongkarn D, Lew JY. Algorithms for real-time estimation of individual wheel tire-road friction coefficients. Mechatronics, IEEE/ASME Transactions on. 2012; 17(6):1183–1195.
[7] Yamada M, Ueda K, Horiba I, Tsugawa S, Yamamoto S. Road surface condition detection technique based on image taken by camera attached to vehicle rearview mirror. Review of automotive engineering. 2005;26(2):163–168.
[8] Sato Y, Kobayashi D, Kageyama I, S T. Study on recognition method for road friction condition. JSAE Trans. 2007;38(2):10471–56.
[9] Eichhorn U, Roth J. Prediction and monitoring of tyre/road friction. In: XXIV FISITA CONGRESS, 7-11 JUNE 1992, LONDON.; 1992. p. –.
[10] Gustafsson F. Slip-based tire-road friction estimation. Automatica. 1997;33(6):1087–1099.
[11] Kayacan E, Oniz Y, Kaynak O. A grey system modeling approach for sliding-mode control of antilock braking system. Industrial Electronics, IEEE Transactions on. 2009;56(8):3244–3252.
[12] Burckhardt M. Fahrwerktechnik: Radschlupf-regelsysteme. Vogel Verlag, Wurzburg. 1993;.
[13] Tanelli M, Savaresi SM. Friction-curve peak detection by wheel-deceleration measurements. In: Intelligent Transportation Systems Conference, 2006. ITSC'06. IEEE. IEEE; 2006. p. 1592–1597.

[14] de Castro R, Araújo RE, Freitas D. Real-time estimation of tyre–road friction peak with optimal linear parameterisation. IET Control Theory & Applications. 2012;6(14):2257–2268.

[15] Qi Z, Taheri S, Wang B, Yu H. Estimation of the tyre–road maximum friction coefficient and slip slope based on a novel tyre model. Vehicle System Dynamics. 2015;53(4):506–525.

[16] Ko S, Ko J, Lee S, Cheon J, Kim H. A study on the road friction coefficient estimation and motor torque control for an in-wheel electric vehicle. Proceedings of the Institution of Mechanical Engineers, Part D: Journal of Automobile Engineering. 2014;:0954407014547750.

[17] Li B, Du H, Li W. Comparative study of vehicle tyre–road friction coefficient estimation with a novel cost-effective method. Vehicle System Dynamics. 2014;52(8):1066–1098.

[18] Sharifzadeh M, Akbari A, Timpone F, Daryani R. Vehicle tyre/road interaction modeling and identification of its parameters using real-time trust-region methods. IFAC-PapersOnLine. 2016; 49(3):111–116.

[19] Sharifzadeh M, Timpone F, Farnam A, Senatore A, Akbari A. Tyre-road adherence conditions estimation for intelligent vehicle safety applications. In: Advances in Italian Mechanism Science: Proceedings of the First International Conference of IFToMM Italy; Vol. 47. Springer; 2016. p. 389–398.

[20] Sharifzadeh M, Farnam A, Senatore A, Akbari A, Timpone F. Road condition monitoring system using the parameters identification of lugre tyre friction model. In: 4th European Conference on Computational Optimization (EUCCO), KU Leuven, Belgium; 2016.

[21] Coleman TF, Li Y. A trust region and affine scaling interior point method for nonconvex minimization with linear inequality constraints. Mathematical Programming. 2000;88(1):1–31.

[22] Moré JJ, Sorensen DC. Computing a trust region step. SIAM Journal on Scientific and Statistical Computing. 1983;4(3):553–572.

[23] Conn AR, Gould NI, Toint PL. Trust region methods. Vol. 1. SIAM; 2000.

[24] Ulsoy AG, Peng H, Çakmakci M. Automotive control systems. Cambridge University Press; 2012.

[25] Hashemi E, Zarringhalam R, Khajepour A, Melek W, Kasaiezadeh A, Chen SK. Real-time estimation of the road bank and grade angles with unknown input observers. Vehicle System Dynamics. 2017; 55(5):648–667.

[26] Akbari A, Lohmann B. Output feedback h_∞/gh_2 preview control of active vehicle suspensions: a comparison study of lqg preview. Vehicle System Dynamics. 2010;48(12):1475–1494.

[27] Farroni F, Russo M, Russo R, Terzo M, Timpone F. A combined use of phase plane and handling diagram method to study the influence of tyre and vehicle characteristics on stability. Vehicle System Dynamics. 2013;51(8):1265–1285.

[28] Petersen I. Wheel slip control in abs brakes using gain scheduled optimal control with constraints. Department of Engineering Cybernetics Norwegian University of Science and Technology, Trondheim, Norway. 2003;.

[29] Pisaturo M, Cirrincione M, Senatore A. Multiple constrained mpc design for automotive dry clutch engagement. Mechatronics, IEEE/ASME Transactions on. 2015;20(1):469–480.

[30] Senatore A, D'Agostino V, Di Giuda R, Petrone V. Experimental investigation and neural network prediction of brakes and clutch material frictional behaviour considering the sliding acceleration influence. Tribology International. 2011;44(10):1199–1207.

[31] Canudas-De-Wit C, Olsson H, Astrom KJ, Lischinsky P. A new model for control of systems with friction. Automatic Control, IEEE Transactions on. 1995;40(3):419–425.

[32] Astrom KJ, Canudas-De-Wit C. Revisiting the lugre friction model. Control Systems, IEEE. 2008; 28(6):101–114.

[33] Yevtushenko A, Adamowicz A, Grzes P. Three-dimensional fe model for the calculation of temperature of a disc brake at temperature-dependent coefficients of friction. International Communications in Heat and Mass Transfer. 2013;42:18–24.

[34] Imsland L, Johansen TA, Fossen TI, Grip HF, Kalkkuhl JC, Suissa A. Vehicle velocity estimation using nonlinear observers. Automatica. 2006;42(12):2091–2103.

[35] Tanelli M, Piroddi L, Savaresi SM. Real-time identification of tire–road friction conditions. IET control theory & applications. 2009;3(7):891–906.

[36] Savino G, Giovannini F, Baldanzini N, Pierini M. Real-time estimation of road–tyre adherence for motorcycles. Vehicle System Dynamics. 2013;51(12):1839–1852.

[37] De Castro R, Araujo RE, Cardoso JS, Freitas D. A new linear parametrization for peak friction coefficient estimation in real time. In: Vehicle Power and Propulsion Conference (VPPC), 2010 IEEE. IEEE; 2010. p. 1–6.

[38] Narendra KS, Xiang C. Adaptive control of discrete-time systems using multiple models. Automatic Control, IEEE Transactions on. 2000;45(9):1669–1686.

21

[39] Li H, Jing X, Lam HK, Shi P. Fuzzy sampled-data control for uncertain vehicle suspension systems. Cybernetics, IEEE Transactions on. 2014;44(7):1111–1126.
[40] Gan M, Li HX, Peng H. A variable projection approach for efficient estimation of rbf-arx model. Cybernetics, IEEE Transactions on. 2015;45(3):476–485.
[41] Pillo G, Roma M. Large-scale nonlinear optimization. Vol. 83. Springer Science & Business Media; 2006.
[42] Gratton S, Sartenaer A, Toint PL. Recursive trust-region methods for multiscale nonlinear optimization. SIAM Journal on Optimization. 2008;19(1):414–444.
[43] Moré JJ. Recent developments in algorithms and software for trust region methods. Springer; 1983.
[44] Tanelli M, Astolfi A, Savaresi SM. Robust nonlinear output feedback control for brake by wire control systems. Automatica. 2008;44(4):1078–1087.
[45] Akbari A, Lohmann B. Multi-objective preview control of active vehicle suspensions. In: 17th IFAC World Congress; 2008.
[46] Akbari A, Lohmann B, Salimbahrami B. Gl2 estimation of front wheel disturbance. In: IFAC World Congress; 2008. p. 10750–10755.

Appendix A. Proof of Lemma 1

The LuGre distributed models (see Fig. 2) can be represented by the following partial differential equation (PDE) and boundary conditions

$$
\begin{cases}
\frac{dz}{dt}(\zeta,t) = v_r - \frac{\theta \sigma_0 |v_r|}{g(v_r)z} \\
F_{xi} = \frac{F_{Ni}}{L} \int_0^L (\sigma_0 z(\zeta,t) + \sigma_1 \dot{z}(\zeta,t) + \sigma_2 v_r)d\zeta
\end{cases}
\tag{A1}
$$

$$
z(0,t) = z(L,t) = 0 \qquad \forall t \geq 0,
$$

Where $z(\zeta,t)$ denotes the corresponding friction state and the patch L represents the projection of the part of the tire that is in contact with the road, with ζ-axis along the length of the patch in the direction of the tire rotation.

$$
\frac{dz}{dt}(\zeta,t) = \frac{\partial z}{\partial t}(\zeta,t) + \frac{\partial z}{\partial \zeta}\dot{\zeta}
\tag{A2}
$$

Assuming that v_v and ω_{wi} are constant, $\dot{\zeta} = |R_w \omega_{wi}|$ and by setting within an small enough interval of time $\frac{\partial z}{\partial t}(\zeta,t) = 0$ applying these conditions in equation A2 gives

$$
\frac{dz}{d\zeta}(\zeta) = \frac{1}{R_w \omega_w i}\frac{dz}{dt}(\zeta,t)
\tag{A3}
$$

$$
\begin{cases}
\frac{dz}{d\zeta}(\zeta) = \frac{v_r}{R_w \omega_w i} - \frac{\sigma_0 |v_r|}{g(\lambda)R_w \omega_{wi}}z, \qquad \zeta \in [0,L] \\
z(\zeta) = \zeta = 0;
\end{cases}
\tag{A4}
$$

Solving the equation A4, one obtains

$$z(\zeta) = \begin{cases} \frac{g(\lambda)}{\sigma_0}\left(exp(-\frac{\sigma_0\lambda\theta}{(1+\lambda)g(\lambda)}\zeta) - 1\right), & 0 \leq \zeta \leq \frac{L}{2} \\ \frac{g(\lambda)}{\sigma_0}\left(exp(-\frac{\sigma_0\lambda\theta}{(1+\lambda)g(\lambda)}(L-\zeta)) - 1\right), & \frac{L}{2} \leq \zeta \leq L \end{cases} \quad (A5)$$

Noticing that $\mu(\lambda_i) = F_{xi}/F_{Ni}$ and Calculating the F_{xi} by term using Equation A1, one obtains

$$F_{xi} = \sigma_0\frac{F_{Ni}}{L}\int_0^L z(\zeta)d(\zeta) + \sigma_1\frac{F_{Ni}}{L}\int_0^L \dot{z}(\zeta)d(\zeta)$$

$$+ \sigma_2 v_r\frac{F_{Ni}}{L}\int_0^L d(\zeta) \quad (A6)$$

$$\Longrightarrow \mu(\lambda_i)$$
$$= \frac{\sigma_0}{L}\left[\frac{Lg(\lambda_i)}{\theta\sigma_0}\left(1 + \frac{2g(\lambda_i)(1+\lambda_i)}{\sigma_0\lambda_i L\theta}(e^{-\frac{\sigma_0\lambda_i L\theta}{2g(\lambda_i)(1+\lambda_i)}} - 1)\right)\right]$$
$$+ \frac{\sigma_1}{L}\left[\frac{2v_v g(\lambda_i)}{\theta\sigma_0}\left(1 - e^{-\frac{\sigma_0\lambda_i L\theta}{2g(\lambda_i)(\lambda_i+1)}}\right)\right] + \sigma_2 v_r \quad (A7)$$
$$\approx \frac{g(\lambda_i)}{\bar{\theta}}\left[1 + \frac{g(\lambda_i)(\lambda_i+1)}{\bar{\theta}\sigma_0\lambda_i L}\left(e^{-\frac{\sigma_0\lambda_i L\bar{\theta}}{g(\lambda_i)(\lambda_i+1)}} - 1\right)\right] + \sigma_2\lambda_i v_v$$

where $g(\lambda_i) = \mu_c + (\mu_s - \mu_c)e^{-\left|\frac{\lambda_i v_v}{v_0}\right|^{1/2}}$